Univerzita Karlova
Přírodovědecká fakulta

Studijní program: Chemie
Studijní obor: Chemie

Eliška Stančíková

Dialýza roztoků polyelektrolytů

Dialysis of polyelectrolyte solutions

Vedoucí práce: doc. RNDr. Peter Košovan, Ph.D.
Konzultant práce: Sebastian Pineda Pineda, M.Sc.

Praha, 2025

Prohlašuji, že jsem závěrečnou práci zpracovala samostatně a že jsem uvedla všechny použité informační zdroje a literaturu. Tato práce ani její podstatná část nebyla předložena k získání jiného nebo stejného akademického titulu.

V Praze dne 17.05.2025 Eliška Stančíková

Abstrakt: Nabité makromolekuly, známé jako polyelektrolyty, se chovají odlišně než jejich neutrální protějšky. Popis složitého chování nabitých polyelektrolytů byl předmětem řady teoretických modelů vyvinutých v průběhu let. Tato práce se zaměřuje na dialýzu roztoků polyelektrolytů, s cílem kvantifikovat Donnanův efekt. Donnanův efekt vychází z nerovnoměrného rozložení iontů mezi roztoky oddělené semipermeabilní membránou, která brání průchodu větších makromolekul. Tato práce usiluje o propojení teoretických modelů s experimentálními pozorováními, čímž přispívá k hlubšímu pochopení chování polyelektrolytů v praktických aplikacích.

Klíčová slova: Dialýza, polyelektrolyty, Donnanův efekt, molekulové simulace

Abstract: Charged macromolecules, known as polyelectrolytes, behave in a distinct way compared to their neutral counterparts. The description of complex behavior of charged poylelectrolytes has been the subject of numerous theoretical models developed over the years. This thesis focuses on the dialysis of polyelectrolyte solutions, with an emphasis on quantifying the Donnan effect. The Donnan effect arises from the unequal distribution of ions across a semipermeable membrane, which restricts the passage to larger macromolecules. By quantifying the Donnan effect and its impact on polyelectrolyte dialysis, this work aims to bridge the gap between theoretical models and experimental observations, contributing to a deeper understanding of polyelectrolyte behavior in practical applications.
Keywords: Dialysis, polyelectrolytes, Donnan effect, molecular simulations

I would thank to my supervisor doc. RNDR. Peter Košovan, Ph.D., for the great opportunity to work on such an interesting topic bridging the experimental and theoretical work, for engaging discussions, opportunities to learn, and support in both moments of doubt and throughout the entire process.

I would also thank to my advisor Sebastian Pineda Pineda, M.Sc. for his invaluable help in setting up the dialysis experiment, scripts for molecular simulations, his continuous support throughout the project, encouragement to strive for the best possible results, for sparking my interest in science and research, and also valuable life advice.

In the end, I would thank to prof. RNDr. Miroslav Štěpánek, Ph.D. for generously providing the polymer essential for this work and for his valuable contributions to the design of dialysis process.

Contents

1 Motivation

Charged macromolecules, known as polyelectrolytes, behave in a distinct way compared to their neutral counterparts. The description of their complex behavior has been the subject of numerous theoretical models developed over the years. Each model relies on specific assumptions and simplifictions, which inevitably limits its accurancy in predicting the behavior of real systems.[1]

This thesis focuses on the dialysis of polyelectrolyte solutions, with an emphasis on quantifying the Donnan effect. The Donnan effect arises from the unequal distribution of ions across a semipermeable membrane, which restricts the passage to larger macromolecules. Membrane separation processes, such as ultrafiltration/diafiltration (UF/DF), are widely used techniques in manufacturing pharmaceutical proteins. These processes rely on principles of selective ion and molecule transport, where the Donnan effect can cause notable differences between the pH and ion concentrations of the retained protein solution and the DF buffer, impacting the quality and stability of the final product.[2]

The primary objective of this thesis is to investigate the Donnan effect in polyelectrolyte solutions using poly(methacrylic acid) (PMAA) under varying conditions, and compare measured pH differences with predictions from ideal Donnan theory and additionally from molecular simulations. Ideal Donnan theory provides useful approximations but has limitations in precision, which is critical in applications such as monoclonal antibody production, where high concentrations demand precise control of solution pH.[2] By quantifying the Donnan effect and its impact on polyelectrolyte dialysis, this work aims to bridge the gap between theoretical models and experimental observations, contributing to a deeper understanding of polyelectrolyte behavior in practical applications.

2 Introduction

2.1 Charged macromolecules

In general, charged macromolecules are formed by linking of many charged monomers to create long polymer chains.[1] This chapter will focus on a limited selection of types of charged macromolecules that are directly related to the topic of this work.

2.1.1 Polyelectrolytes

Polyelectrolytes are macromolecules that can dissociate in water, resulting in distributed ionized groups along the chain. In equilibrium, the polyelectrolyte solution must remain electrically neutral with the number of counterions equal to the number of charges on the polyelectrolyte chain in the solution.[3, 4]

The behavior of polyelectrolytes is affected by the properties of both the polymer and the ions present in the solution.[1] In particular, the ionized groups within the polyelectrolyte chains interact with each other under the influence of the Coulomb potential.[5] Their conformation is determined by the Coulomb interaction between two charges q_i and q_j separated by a distance r_{ij} and can be expressed as the Coulombic potential energy U [6]:

$$U = \frac{q_i q_j}{4\pi\epsilon_0\epsilon_\mathrm{r} r_{ij}} \tag{2.1}$$

where ϵ_0 is permittivity of vacuum and ϵ_r is the relative permittivity of medium. The distance at which the Coulomb potential energy between two elementary charges e is equal to thermal energy $k_\mathrm{B}T$, is called as the Bjerrum length λ_B[7]:

$$\lambda_\mathrm{B} = \frac{e^2}{4\pi\epsilon_0\epsilon_\mathrm{r} k_\mathrm{B} T} \tag{2.2}$$

where k_B is the Boltzmann constant, T is temperature.

Additionally, small ions present in the solution affect the interaction between charged groups on the polyelectrolyte. As the ionic strength of a solution increases with added salt, Coulomb forces are more effectively screened by ions, depending on their concentration and type. As a result, at high ionic strength, the charges on the polyelectrolyte chain are more screened, which leads to the contraction of the polymer molecule compared to a salt-free solution. On the other hand, at low ionic strength, reduced screening allows stronger electrostatic repulsion between charged groups resulting in more expanded structure. The conformation of polylelectrolyte chain is also influenced by the excluded volume interaction between two monomers. Each occupies a specific volume limiting the approach of another monomer.[1, 8, 9]

Weak polyelectrolytes

As mentioned above, polyelectrolytes carry ionizable groups that can dissociate in water. These groups are either acidic or basic. Similar to monomeric acids

and bases are classified as strong or weak, the degree to which a polyelectrolytes dissociate determines their classification. Strong polyelectrolytes completely dissociate in a solution over a wide range of pH, unlike weak polyelectrolytes, whose dissociation depends on the pH. This subsection will be limited to weak polyacids which consist of weakly acidic groups.[3, 10] The dissociation of the groups is represented by the following reaction

$$\mathrm{HA} \rightleftarrows \mathrm{H}^+ + \mathrm{A}^- \tag{2.3}$$

resulting in a formation of H^+ and the ionized form of the acid c_{A^-}. This process is quantified by the degree of ionization, that is defined by the equation

$$\alpha = \frac{c_{\mathrm{A}^-}}{c_{\mathrm{A}^-} + c_{\mathrm{HA}}} \tag{2.4}$$

where c_{A^-} refers to the equilibrium concentration of c_{A^-} groups, while c_{HA} represents the equilibrium concentration of c_{HA} groups. The ionization degree can be related to pH by the Henderson-Hasselbach equation

$$\log_{10} \frac{\alpha}{1-\alpha} + \mathrm{p}K_{\mathrm{A}} = \mathrm{pH} \tag{2.5}$$

where $\mathrm{p}K_{\mathrm{A}}$ corresponds to the acidity constant and is defined by the equation [11, 12]:

$$\mathrm{p}K_{\mathrm{A}} = -\log_{10} K_{\mathrm{A}} \tag{2.6}$$

At $\mathrm{pH} \gg \mathrm{p}K_{\mathrm{A}}$, the degree of ionization approaches 1. At high pH values, where $\alpha \approx 1$, weak polyacids exhibit behavior similar to that of strong polyacids, due to near-complete ionization.

Charge regulation

In aqueous solutions containing polyelectrolytes, each molecule interacts with every other molecule present in the system. In this context, an important characteristic of polyelectrolytes is charge regulation, which refers to a change in the charge state of a molecule in response to its local environment, for example, the change of pH and salt concentration.[1, 13]

The HH equation (Equation 2.5) cannot be used for polyelectrolytes, as their titration curves qualitatively differ from those of their corresponding monomers. The ionization of weak polyelectrolytes is better described by an effective acidity constant $\mathrm{p}K_{\mathrm{eff}}$, that depends on ionization degree, polymer chain length and concentration as well as ionic strength and reflects non-ideal behavior of specific system and conditions The effective acidity constant can be derived from experimentally measured α and is defined as follows[14]:

$$\mathrm{p}K_{\mathrm{eff}} = \mathrm{pH} + \log_{10}\left(\frac{1-\alpha}{\alpha}\right) \tag{2.7}$$

To reduce electrostatic repulsions among ionized groups of the same charge, polyelectrolytes can regulate the local charge of the ionized groups to decrease the total (net) charge on the chain. This, in turn, causes a change in the effective acidity constant, $\mathrm{p}K_{\mathrm{eff}}$ of weak polyacids to higher values that eventually differ from the $\mathrm{p}K_{\mathrm{A}}$ of the corresponding monomer.[13]

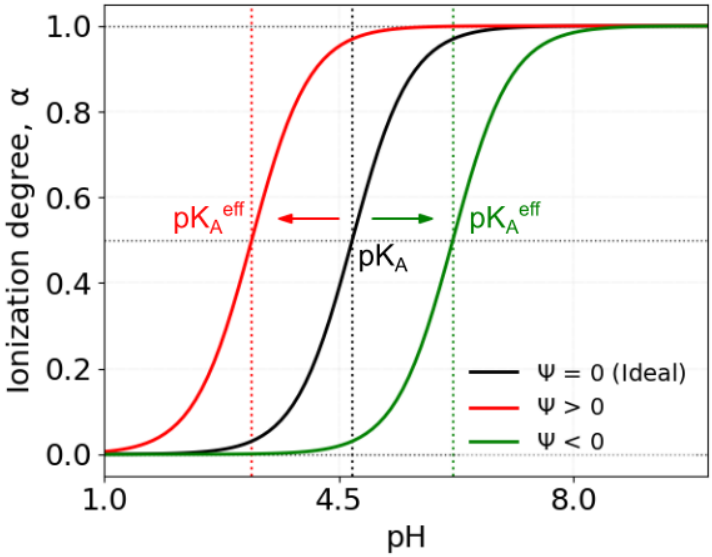

Figure 2.1 The shift in $\mathrm{p}K_{\mathrm{eff}}$ from $\mathrm{p}K_{\mathrm{A}} = 4.7$ corresponding to the monomer of PMAA[15] depending on the value of local electrostatic potential Ψ, where $\Psi > 0$ indicate electrostatic attraction between ionizable groups, whereas $\Psi < 0$ indicate electrostatic repulsions between the groups. Adapted from a similar figure authored by my advisor Sebastian Pineda Pineda.

The local electrostatic potential Ψ governs interactions between ionizable groups on polyelectrolyte chain: $\Psi > 0$ indicates electrostatic attractions, while $\Psi > 0$ indicates repulsion between the groups. In relation to the $\mathrm{p}K_{\mathrm{A}}$ of corresponding monomer the $\mathrm{p}K_{\mathrm{eff}}$ is given by:

$$\mathrm{p}K_{\mathrm{eff}} = \mathrm{p}K_{\mathrm{A}} + \frac{e\Psi}{k_{\mathrm{B}}T} \tag{2.8}$$

where e is the elementary charge. The shift from the $\mathrm{p}K_{\mathrm{A}}$ corresponding to the monomer of the polyelectrolyte used in this thesis[15], PMAA depending on the value of local electrostatic potential Ψ is showed in Figure 2.1.

2.1.2 Proteins

In many biological systems, polyelectrolytes in electrolyte solutions play an important role. For instance, DNA, RNA and proteins – charged macromolecules – are often found in aqueous solutions containing simple ions.[16]

Proteins are usually linear heteropolymers composed of different amino acid monomeric units, connected by peptide bonds. Depending on the type of amino acid, monomeric units can be acidic, basic, neutral, and hydrophobic. Because the acidic and basic groups undergo dissociation reactions, the net charge and distribution of charges in protein molecules are heavily influenced by their environment.[1] In molecules that have acidic and basic groups, the net charge and distribution of the groups in the protein can cause a shift in the effective $\mathrm{p}K_{\mathrm{A}}$ in one direction or another.[17]

In addition to naturally occurring proteins, recombinant proteins (artificially produced proteins) such as monoclonal antibodies, have become very important

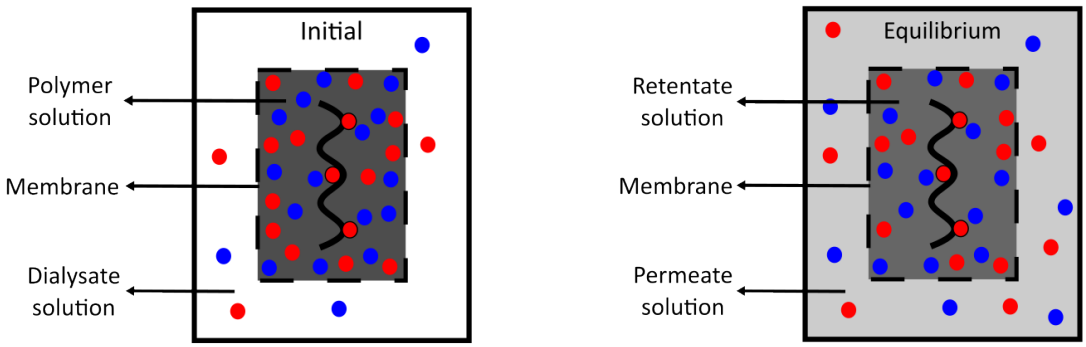

Figure 2.2 Schematic illustration of the dialysis setup, showing the initial state with a polymer and dialysate solution separated by a semipermeable membrane, and the equilibrium state with retentate and permeate solution. Adapted from a similar figure authored by my advisor Sebastian Pineda Pineda.

in biopharmaceutical field. These engineered proteins are designed for treatment and prevention of numerous diseases and require high protein concentration, often greater than 100 g/L. These protein solutions are concentrated to these high values using membrane separations processes, while removing small solutes.[2, 8, 18]

2.2 Membrane separation processes

In industrial membrane separation processes, ultrafiltration and diafiltration are among the most widely used techniques.[19] Before ultrafiltration membranes became available, dialysis was the standard laboratory method for purifying biological solutions.[19] Although the mechanisms of the separation methods differ, ultrafiltration and diafiltration are conceptually similar to dialysis. All use semipermeable membrane to selectively allow passage of small molecules and ions while retaining larger molecules. However, unlike dialysis, which relies on a concentration gradient (difference in concentration across a given distance), both ultrafiltration and diafiltration are pressure-driven techniques.[6, 19]

2.2.1 Dialysis

Dialysis serves as an important example of osmosis – the diffusion of solvent molecules through a semipermeable membrane due to the difference in concentrations. Osmotic pressure, defined by the van't Hoff equation, is the pressure difference between the two sides of the membrane that controls the flow of sol-

vent[6]:

$$\Pi = \frac{nRT}{V} \tag{2.9}$$

where n represents number of moles of solute, R is the universal gas constant ($8.314\,\mathrm{JK^{-1}mol^{-1}}$), T is absolute temperature and V is the volume of the pure solution.

In the initial state of dialysis, the polymer solution, and the dialysate are separated by a semipermeable membrane. During dialysis, small molecules and ions diffuse across the membrane to maintain electroneutrality, while the larger polymer chains are retained. In this thesis, at equilibrium, the retained solution is referred to as the retentate and the outer solution as the permeate, as illustrated in Figure 2.2.

The chemical potential μ_S of the dissolved solute S is related to its activity by:

$$\mu_\mathrm{S} = \mu_\mathrm{S}^\circ + RT\ln a_\mathrm{S} \tag{2.10}$$

where μ_S° is the standard chemical potential and a_S is the activity of S, which is the effective concentration of a solute:

$$a_\mathrm{S} = \gamma_\mathrm{S}\frac{c_\mathrm{S}}{c^\circ} \tag{2.11}$$

where γ_S is the activity coefficient of S, c_S is the concentration of S and c° is the standard concentration (equal to $1\,\mathrm{mol/L}$). In dialysis, the system reaches equilibrium when the chemical potential of S becomes equal in both solution phases, retentate ret and permeate perm, separated by the semipermeable membrane[6]:

$$(\mu_\mathrm{S})^\mathrm{ret} = (\mu_\mathrm{S})^\mathrm{perm} \tag{2.12}$$

At equilibrium, the chemical potentials are related by:

$$(\mu_\mathrm{S}^\circ)^\mathrm{ret} + RT\ln a_\mathrm{S}^\mathrm{ret} = (\mu_\mathrm{S}^\circ)^\mathrm{perm} + RT\ln a_\mathrm{S}^\mathrm{perm} \tag{2.13}$$

where μ_S° is the standard chemical potential for the solute, which is equal in phases ret and perm. As a result, the activities $a_\mathrm{S}^\mathrm{ret}$ and a_S^perm are also equal at equilibrium.[20]

2.2.2 Ultrafiltration

Ultrafiltration (UF) is used for concentrating solutions containing dissolved macromolecules, such as proteins, by separating them from smaller particles or molecules. Ultrafiltration depends on the pore size of the membrane, which is smaller than the molecular weight of targeted macromolecules, retaining them for separation from the smaller components of the solution, that are allowed to pass through the membrane. It has a wide range of applications, one of which is the concentration and purification of target biomolecules, like proteins or DNA.[19, 21]

2.2.3 Diafiltration

After purifying the target protein from smaller particles and molecules of the solution, diafiltration (DF) is used to further separate the target protein from other components in the solution with similar sizes. Typically, both steps are carried out together in a combined ultrafiltration/diafiltration (UF/DF) process. [2, 19]

During DF, partially permeable proteins are gradually washed out from the protein solution through the membrane, typically by replacing the solution with a DF buffer, while the proteins that cannot pass through are retained. The permeate solution is then reconcentrated by UF with a membrane retaining all proteins. Finally, a second DF step is performed to separate the target protein from the unwanted components in the solution, from the reconcentrated permeate solution. [2, 19]

2.3 Donnan effect

When a polyelectrolyte solution is separated by a semipermeable membrane from a salt solution, small ions redistribute across the membrane to maintain electroneutrality, while the polyelectrolyte ions remain inside the membrane. At equilibrium, the concentration of small cations and anions (such as H^+, OH^-, Na^+ and Cl^-) in the retentate either increases or decreases compared to the initial state, while their concentration in the permeate adjusts to maintain electroneutrality. The final difference in concentrations occur due to the Donnan effect.

The resulting distribution of small ion i across the membrane can be described by distribution ratio[22]:

$$D_i = \frac{c_i^{\text{ret}}}{c_i^{\text{perm}}} \tag{2.14}$$

where c_i^{ret} and c_i^{perm} are the concentrations of i ion in the retentate and permeate, respectively.

Generally, the distribution ratio of ions in relation to theelectrostatic potential Ψ is given by:

$$D = \exp(\frac{z\Psi e}{k_{\text{B}}T}) \tag{2.15}$$

where z is the charge of the ion. The distribution ratios of monovalent cations ($z = +1$) are equal in the ideal case, since the ratio of concentrations of monovalent cations such as $Na^+$is directly proportional to that of H^+. In contrast, in the ideal case, the distribution ratios of monovalent anions ($z = -1$) are inversely proportional to those of the cations. Therefore[11]:

$$D_+ = D_{\text{H}^+} = D_{\text{Na}^+} = \frac{1}{D_-} = \frac{1}{D_{\text{OH}^-}} = \frac{1}{D_{\text{Cl}^-}} \tag{2.16}$$

The distribution ratio of H^+ions can be related to pH, which is given by:

$$\text{pH} = -\log_{10} a_{\text{H}^+} = -\log_{10} \frac{\gamma_{\text{H}^+} c_{\text{H}^+}}{c^\circ} \tag{2.17}$$

where a_{H^+} is the activity of hydrogen ions.

The difference in pH between the retentate and permeate is defined as:

$$\Delta\mathrm{pH} = \mathrm{pH}_{\mathrm{ret}} - \mathrm{pH}_{\mathrm{perm}} \tag{2.18}$$

This difference can be expressed in terms of the activities of H^+ions in both phases:

$$\Delta\mathrm{pH} = -\log_{10} \frac{a_{\mathrm{H}^+}^{\mathrm{ret}}}{a_{\mathrm{H}^+}^{\mathrm{perm}}} \tag{2.19}$$

By substituting the formula for activity:

$$\Delta\mathrm{pH} = -\log_{10} \frac{\gamma_{\mathrm{H}^+}^{\mathrm{ret}} c_{\mathrm{H}^+}^{\mathrm{ret}}}{\gamma_{\mathrm{H}^+}^{\mathrm{perm}} c_{\mathrm{H}^+}^{\mathrm{perm}}} \tag{2.20}$$

If the activity coefficients of hydrogen ions in the retentate and permeate are approximately equal

$$\frac{\gamma_{\mathrm{H}^+}^{\mathrm{ret}}}{\gamma_{\mathrm{H}^+}^{\mathrm{perm}}} \approx 1 \tag{2.21}$$

the Equation 2.20 could be simplified to:

$$\Delta\mathrm{pH} = -\log_{10} \frac{c_{\mathrm{H}^+}^{\mathrm{ret}}}{c_{\mathrm{H}^+}^{\mathrm{perm}}} \tag{2.22}$$

Due to the Donnan effect, during UF/DF processes of charged protein solutions, their pH can shift significantly from the value set in the DF buffer.[23] Predicting the difference between pH of the retentate and the permeate is a major challenge in protein purification and can be modeled using simple analytical models[2] or models based on Poisson-Boltzmann theory.[24]

2.4 Molecular simulations

Although results from molecular simulations are used in this work, they are not the primary focus of this thesis. In the following section, the basic principles are briefly mentioned to provide the necessary context.

To predict the behavior of isolated polyelectrolyte chains remains a significant challenge by simple models. Specifically, because their size, counterion distribution and changes in electric potential within and around the polymer coils, cannot be measured directly. Instead, these characteristics are concluded from measurements of other features, whose interpretation relies strongly on accurate theoretical descriptions. In this regard, molecular simulations have proven to be a valuable tool for understanding how charges behave in polyelectrolyte solutions.[1]

2.4.1 Simulation models

Before performing a simulation, a suitable model must be chosen that accurately reflects the behavior of the real system. To model complex systems like polyelectrolytes, the two main groups of models include atomistic and coarse-grained models. Atomistic models describe the system in detail by simulating each atom explicitly. However, their use remains impractical for complex systems

such as proteins and polymers, especially due to high computational demands. In contrast, coarse-grained (CG) models have gained prominence over the last years, offering broader description than classical atomistic models. In CG models, beads represent groups of atoms or number of monomeric units, reducing the computational demands while aiming to preserve the key parameters of the system. [25–27]

2.4.2 The Grand Reaction Monte Carlo Method

The Grand Reaction Monte Carlo Method (G-RxMC), developed by Landgesell *et al.* [24, 28], is applied to study acid-base equilibria in a two-phase system, where charged macromolecules are located in one phase (system) interacting with the other phase (reservoir). In dialysis, poylelectrolyte is restricted to the system phase by a semi-permeable membrane, whereas small ions can transfer without constraint across the semi-permeable membrane to maintain electroneutrality (see also Section 2.3).

In the simulated system for dialysis, the system contains a weak polyelectrolyte consisting of ionizable groups, that undergo dissociation. In the case of weak polyacid, the dissociation involves H^+ ions. As mentioned above, the presence of polyelectrolyte alters how ions are distributed between the retentate and permeate. The distribution of H^+, in turn, influences the ionization equilibrium of the polyelectrolyte. Apart from the Donnan effect, the presence of charged monomeric units along the polyelectrolyte chain suppresses their ionization. This occurs due to strong electrostatic repulsion between like charges, which shifts the equilibrium towards the uncharged form of the monomeric units.[14, 24, 29]

In the G-RxMC, the reservoir is assumed to be sufficiently bigger than the system, meaning that the ionic composition of the reservoir remains constant despite the exchange of ions with the system, which reflects the conditions of dialysis. The composition of the reservoir is defined by the chemical potentials of the small ions it contains, and ion exchange between the system and reservoir occurs through the insertion and removal of electroneutral ion pairs. This ensures, that in result, the chemical potentials of all small ions are equal in the system and reservoir. This exchange is defined by the following reaction involving ion pairs consisting of ions such as Na^+, Cl^-, H^+ and OH^-. The following reactions define the insertion of ion pairs[11, 24, 30]:

$$\emptyset \rightleftharpoons Na^+ + Cl^- \tag{2.23}$$

$$\emptyset \rightleftharpoons H^+ + Cl^- \tag{2.24}$$

$$\emptyset \rightleftharpoons Na^+ + OH^- \tag{2.25}$$

$$\emptyset \rightleftharpoons H^+ + OH^- \tag{2.26}$$

where $\emptyset$ symbolizes an empty set. In the forward reaction, $\emptyset$ corresponds to the insertion of an ion pair in the system, whereas in the backward reaction, an ion pair is removed from the system.

To account for non-ideal behavior arising from interactions in the system, it is necessary to include activity coefficients that is related to the equilibrium constant K_{ij} - for each ion pair ij is defined by the equation[30]:

$$K_{ij} = \frac{\gamma_{\pm}^2 c_i^{\text{res}} c_j^{\text{res}}}{(c^{\ominus})^2} \tag{2.27}$$

where c^{res} corresponds to concentration in the reservoir, i and j refer to each ion of the ion pair and $\gamma_{\pm} = \sqrt{\gamma_i \gamma_j}$ is the mean activity coefficient.

3 Aims of the thesis

The primary goal of this thesis is to experimentally quantify the Donnan effect from dialysis of polyelectrolyte solutions, with a focus on developing an experimental protocol and examining the behavior of PMAA under varying conditions. Dialysis was selected for its simpler experimental setup compared to more complex industrial membrane separation processes. PMAA was chosen as the model polyelectrolyte due to its ready availability and inexpensive cost, making it a practical choice for this study. Proteins are significantly more expensive and complex – by first investigating the Donnan effect in PMAA solutions, we can develop and validate our experimental and theoretical approaches using simpler and cheaper system. The experimental results will be compared with the predictions from ideal Donnan theory and molecular simulations to evaluate their precision. However, molecular simulations are not the primary focus of this thesis. The specific aims were:

- Develop and validate a protocol for dialysis of a polyelectrolyte solution, ensuring reliable and reproducible measurement of pH differences.
- Quantify the Donnan effect from dialysis of PMAA at different pH values and ionic strength.
- Compare experimental values of ΔpH with theoretical predictions from ideal Donnan equilibrium theory and with predictions from molecular simulations of ideal and interacting systems.

By achieving these objectives, this thesis aims to enhance the understanding of polyelectrolyte behavior in membrane separation processes.

4 Materials and methods

4.1 Materials

4.1.1 Poly(methacrylic acid)

The polymer used in this thesis was poly(methacrylic acid) (PMAA), purchased from Polysciences, Inc., with molecular weight $\sim$ 100 000 g/mol, as reported by the manufacturer. The dispersity was not specified, however, for our experiments was not required, as the calculations did not depend on the polymer's molecular weight. For PMAA to be retained by the membrane, its molecular weight must be significantly higher than the membrane's molecular weight cut-off (MWCO).

PMAA consists of ionizable carboxyl groups, which carry charge, depending on the pH. The reported pK_{A} value of the PMAA is typically around 4.7[31], though values vary across references. However, the effective acidity constant pK_{eff} of the PMAA polymer depends on factors such as molecular size and solution conditions, influencing its ionization behavior.[14]

4.1.2 Other chemicals

Milli-Q water was produced by the Barnstead MicroPure water purification system (Thermo Scientific).

NaCl was purchased from Lach-Ner, s.r.o. (99.97 % purity) and from SIGMA-ALDRICH s.r.o. ($\geq$ 99.5 % purity).

Solutions of HCl and NaOH were prepared using ampoules intended for the preparation of 1000 mL 0.1 M volumetric solutions, purchased from Penta s.r.o.

4.2 Equipment

4.2.1 Membranes

Dialysis experiments were performed using semipermeable membranes Spectra/Por 3 (Spectra Laboratories Inc.) with 3.5 kDa molecular weight cut-off (MWCO). They were wetted by stirring in deionized water for 30 minutes to remove the preservative, then rinsed thoroughly with deionized water and placed in a 0.1 % aqueous solution of sodium azide for storage. The role of sodium azide is to prevent bacterial growth. Before dialysis, membranes were rinsed and conditioned as described in Section 4.3.2.

4.2.2 Titrator

The adjustment of pH and titrations were performed on a Metrohm 888 Titrando Compact titrator equipped with a magnetic stirrer, a Pt1000 temperature sensor and LL Biotrode 3.0 mm glass electrode for measuring pH, was used for pH adjustment and automated titrations. The titrator is programmable, allowing to customize methods of pH adjustment or control of added volume of stock solution.

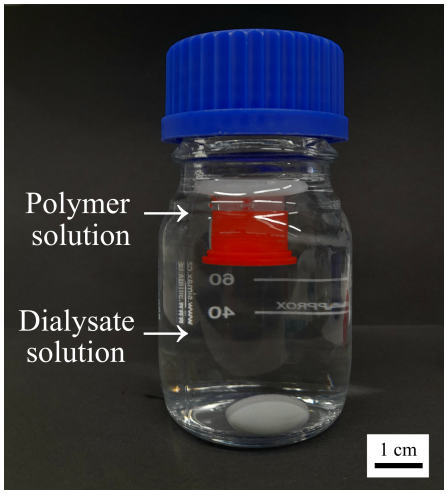

(a) Dialysate solution is in a closed bottle separated by a semipermeable membrane from a polymer solution in a lidded container.

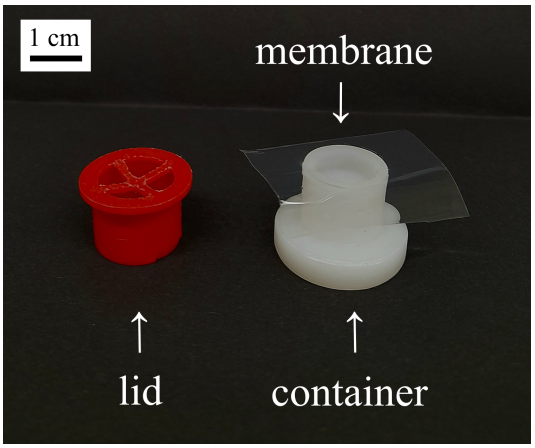

(b) Polymer solution in a container and semipermeable membrane placed on top, next to a lid.

Figure 4.1 Two configurations: a dialysis setup with a magnetic stirrer (a) and dialysis setup of the polymer solution (b).

For data collection and manual control of the titrator, Titrando software "tiamo" was used.

4.3 Methods

4.3.1 Experimental setup for dialysis

Dialysis was carried out using an experimental setup consisting of the sample container holding the polymer solution, separated by a semipermeable membrane from the dialysate solution, as shown in Figure 4.1a. Figure 4.1b shows a close picture of the sample container, which consists of a container for the polymer solution, the membrane positioned on top of it and the enclosing lid.

4.3.2 Optimization of the dialysis protocol

To ensure reliable and reproducible results from dialysis experiments, numerous aspects of the protocol were optimized in the process. This included determining the time required to reach equilibrium, minimizing carbonization effects and introducing a membrane rinsing procedure, and optimizing the pH conditions for polymer and dialysate solutions. These optimizations were the most time-consuming part of the experimental work.

Dialysis duration

Preliminary experiments were performed to determine the time required for the system to establish equilibrium. In total, 8 dialysis setups were prepared. For that, PMAA solutions at concentration 1 g/L were dialyzed against a 10^{-3} M NaCl dialysate solution. The initial pH for both the polymer and dialysate solutions

were set to 10. The pH of the retentate and permeate solutions was measured for each setup over 4 days and the measurements were taken every 12 hours. First setup pH was measured after 12 hours, the second after next 12 hours and so on for all eight samples. Based on the results discussed in Section 5.3.2, a duration of 72 hours was selected for the subsequent experiments.

Initial dialysis experiments

Initial dialysis experiments were conducted to explore the effect of different pH on dialysis using PMAA solutions at a low degree of ionization – PMAA dissolved in water resulting in pH values around 3. Then, NaOH was added to set the pH to 4. The pH of the dialysate was set to pH around 10. These conditions produced results that were consistent with the ideal Donnan theory. For the data not shown, further experiments working with initial pH values of the polymer solution, where the PMAA degree of ionization was lower than 1, led to several challenges interpreting the results due to uncertainties in determining PMAA's ionization degree. Additional difficulties arose from inconsistent pH stability in the dialysate at high pH, requiring further optimization.

To eliminate the uncertainty in the ionization degree of PMAA at pH values where the degree of dissociation α is less than 1, we performed experiments with the initial pH of both the polymer solution and the dialysate set to 10, where the ionizable groups on the polymer chain could be considered fully ionized.

Uptake of atmospheric CO_2

During the preparation of NaCl dialysate solutions at high pH, a decrease in measured pH was observed corresponding to an uptake of atmospheric CO_2 (carbonization). This was significant in solutions stored with larger air volumes. To minimize this effect, solutions were stored in nearly full, tightly sealed bottles and handled minimally when exposed to air. This reduced the pH drift due to carbonization.

Rinsing of the membrane

Additionally, a rinsing step for the membrane was introduced to further minimize the the inconsistent pH stability in the dialysate at high pH. Aside from standard rinsing to remove residual azide, the membrane was submerged in NaCl solution intended for the permeate and reserved during the rest of the setup before dialysis.

4.3.3 Dialysis protocol

To perform dialysis, a series of NaCl dialysate solutions with defined concentrations were dialyzed against PMAA solutions of concentrations 10 g/L and 1 g/L. To ensure reliability of the experimental setup and consistency of the measured pH values, all dialysis preparations were performed in duplicate. Dialysate and polymer solutions were prepared using Milli-Q water.

Preparation of dialysate solutions

Dialysate solutions with concentrations of 10^{-3} M, 10^{-2} M and 10^{-1} M NaCl were prepared by diluting a concentrated stock solution. First, 1 M NaCl stock solution was prepared by dissolving solid NaCl. Afterwards, the 1 M NaCl solution was diluted to the desired working concentrations.

For pH adjustment, 0.1 M NaOH solution was used. Most of the estimated NaOH volume was added beforehand from the titrator in manual mode, and then the titrator was used in an automated mode to adjust the pH precisely. All solutions were stored in tightly closed bottles to avoid carbonization.

Preparation of polymer solutions

The polymer solutions were prepared so as to reach the final PMAA concentration of 1 g/L and 10 g/L. Slightly different approach was used for preparation at each concentration, due to the increasing buffering capacity of PMAA at higher concentration, which affected the pH adjustment process. For both cases, the required amount of PMAA was dissolved in approximately 90 % of the total volume of solution and left to dissolve overnight to allow full dissolution. The remaining volume was added next day, using the titrator in automated mode to adjust the pH to the desired value. All solutions were stored in tightly closed flasks to avoid carbonization.

Dialysis sample setup

The sample setup consisted of the sample container holding the polymer solution, separated by a semipermeable membrane from the dialysate, as illustrated in Figure 4.1a. A blank setup, containing only dialysate without polymer, was also used for comparison.

The dialysate solution was stirred at 300 rpm using a magnetic stirrer. The pH values of both the polymer and dialysate solutions were measured before the start of dialysis and after 72 hours.

The ionic strength the permeate solution, I_{perm}, was calculated for each system using the following equation:

$$I_{\mathrm{perm}} = \frac{1}{2}\sum(c_i z_i^2) \tag{4.1}$$

where c_i is the concentration and z_i is the charge of each ion, contributing to the ionic strength. The calculation accounted for the concentration of NaCl (where $c_{\mathrm{NaCl}} = [\mathrm{Na}^+] = [\mathrm{Cl}^-]$) and the concentration of OH^- ions, which was calculated from the pH of permeate at equilibrium using the expression $[\mathrm{OH}^-] = 10^{-(14-\mathrm{pH}_{\mathrm{perm}})}$. The contribution of H^+ ions was neglected due to its minor magnitude at pH $\approx$ 10.

4.3.4 Calculation of theoretical values

The theoretical values for the system described above were calculated based on the ideal Donnan theory to predict ΔpH between the retentate and permeate. The ionic strength of the permeate solution was calculated using the same approach as for the experimental ionic strength, as described in Section 4.3.3.

The distribution ratio of cations, D_+, representing the concentration ratio of small cations between retentate and permeate, was calculated using:

$$D_+ = \frac{c_+^{\text{ret}}}{c_+^{\text{perm}}} = \frac{c_{\text{A}^-}}{2I_{\text{perm}}} + \sqrt{(\frac{c_{\text{A}^-}}{2I_{\text{perm}}})^2 + 1} \tag{4.2}$$

where $c_{\text{A}^-}$is the concentration of the ionized form of the acidic groups of the poylelectrolyte (PMAA) in the retentate, related to the total PMAA concentration c_{A} by:

$$c_{\text{A}^-} = \alpha c_{\text{A}} \tag{4.3}$$

Here, c_{A} represents the total concentration of PMAA monomeric units, with c_{A^-} being the ionized form and $c_{\text{HA}} = (1-\alpha)c_{\text{A}}$ as the non-ionized form. The degree of ionization is defined by Equation 2.4 and assumed to be $\alpha \approx 1$ at pH ≥ 10 based on the titration data (Section 5.1). The ΔpH was then calculated as:

$$\Delta\text{pH} = -\log D_+ \tag{4.4}$$

indicating the pH difference between retentate and permeate caused by the Donnan effect.

For context, under conditions where the polyelectrolyte concentration significantly exceeds the ionic strength ($c_{\text{A}^-} \gg I_{\text{perm}}$), Equation 4.2 can be simplified to[11]:

$$D_+ \approx \frac{c_{\text{A}^-}}{I_{\text{perm}}} \tag{4.5}$$

Additionally, the ideal Henderson-Hasselbalch (HH) equation (2.5) relates the pH of retentate, pH_{ret}, to the degree of ionization:

$$\log_{10} \frac{\alpha}{1-\alpha} + \text{p}K_{\text{A}} = \text{pH}_{\text{ret}} \tag{4.6}$$

Incorporating the Donnan effect, this can be modified to account for the permeate pH (pH_{perm}) and ΔpH:

$$\log_{10} \frac{\alpha}{1-\alpha} + \text{p}K_{\text{A}} = \text{pH}_{\text{perm}} + \Delta\text{pH}(\alpha) \tag{4.7}$$

While Equations (4.5) - (4.7) provide useful approximations and alternative formulations, the theoretical ΔpH values in this work were calculated directly from Equations (4.1) - (4.4), using ionic strength I_{perm} consistent with the experimental conditions.

4.4 Potentiometric titration

To obtain titration curves and determine the dependence of the ionization degree of PMAA on pH, potentiometric titrations were performed. The titrations were carried out using PMAA solutions at concentrations of 1 g/L and 10 g/L.

For each titration, 2.0 mL of the PMAA solution was transferred to the titration vessel and titrated with 0.1 M NaOH solution until the pH reached approximately 12.5. For the titration of 1 g/L PMAA, 0.1 mL of 0.1 M HCl was added before the titration, to adjust the pH to a lower value. For the titration of 10 g/L PMAA,

no HCl was added beforehand. To minimize CO_2 absorption during the titration, the titration vessel was kept under soda lime.

Additionally, the dependence of degree of ionization of the PMAA as a function of solution pH was obtained from titration data. The measured pH values and the volume of NaOH added, provided by the titrator, were processed using a Python script that extracted the data and generated the corresponding plots.

The degree of ionization was calculated based on the charge of the monomeric unit, z_{mon}, expressed in units of the elementary charge e, according to the following equation:

$$z_{\text{mon}} = \frac{n_{\text{HCl}} - n_{\text{NaOH}} + n_{\text{H}^+} - n_{\text{OH}^-}}{n_{\text{mon}} c_{\text{factor}}} \tag{4.8}$$

where n_{HCl}, n_{NaOH}, n_{H^+} and n_{OH^-} represent the amounts in moles of HCl, NaOH, H^+, and OH^-, respectively, and n_{mon} is the number of moles of monomeric units.

Finally, the degree of ionization, α, was calculated as:

$$\alpha = z_{\text{mon}} / z_{\text{max}} \tag{4.9}$$

where z_{max} is the maximum charge of a monomeric unit, equal to -1 for PMAA.

The concentration factor c_{factor} was introduced to scale the dependence of α on pH, as pH measurements alone cannot distinguish the specific charges of ionized groups in the polyelectrolyte. c_{factor} was set to a value 0.85.

4.5 Molecular simulations

4.5.1 System description

The simulated system includes a weak polyelectrolyte (retentate) solution in equilibrium with a permeate solution of specific pH and salt concentration. The weak polyelectrolyte, in this case consisting of acidic groups, undergoes dissociation involving H^+ ions and remains in the retentate, while small ions move freely between the retentate and the permeate, as shown in Figure 4.2. As a result of the Donnan equilibrium, the pH and concentration of small ions differ between the two compartments. [24]

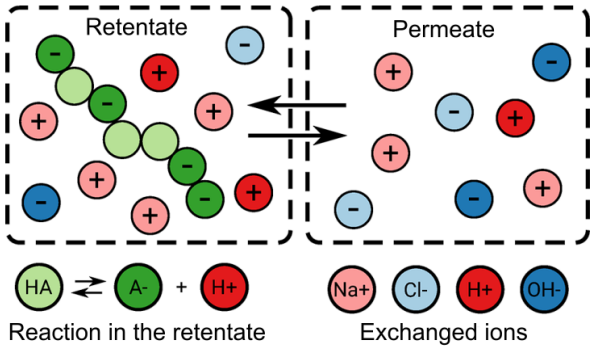

Figure 4.2 The scheme of the simulated system consisting of a weak polyelectrolyte solution and permeate solution at equilibrium. Adapted from Landsgesell et al., *Macromolecules*, 2020, **53** (7), 3009–3021. © 2020 American Chemical Society. [24]

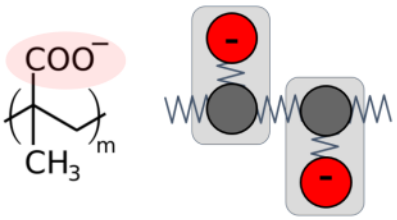

Figure 4.3 The scheme of a two-bead model of PMAA with m monomeric units, used with kind permission from my advisor Sebastian Pineda Pineda.

4.5.2 Simulation model

A dialysis equilibrium between the simulation box with a PMAA solution (retentate) coupled to a virtual reservoir with small ions (permeate), was simulated using a coarse-grained bead-spring (CG-BS). The model features an implicit solvent and includes explicit ions. The PMAA was represented by two-bead model, where each monomeric unit consists of a central backbone bead and a side chain carrying the ionizable group, as illustrated in the Figure 4.3.

In the model, PMAA was represented as a single polymer chain composed of 50 monomeric units, with pK_{A} value set to 4.7. Following this, the titration curve for PMAA was modeled to study its ionization behavior at different pH values. Apart from PMAA, small ions Na^+, $Cl^-$and H^+, OH^- were included in the system to establish different ionic strengths I equal to 10^{-3}, 10^{-2} and 10^{-1} M.

Every bead displayed excluded volume interactions, represented through the conventional Weeks-Chandler-Andersen (WCA) potential model defined by equation:

$$U_{\mathrm{WCA}}(r) = \begin{cases} 4\epsilon \left[\left(\frac{\sigma}{r}\right)^{12} - \left(\frac{\sigma}{r}\right)^{6} + \frac{1}{4} \right] & r \leq r_{\mathrm{cut}} \\ 0 & r > r_{\mathrm{cut}} \end{cases} \tag{4.10}$$

where r is the bond length, ϵ is the depth of the potential well, σ is the effective size of particle and r_{cut} is the cutoff distance at which the interaction disappears. For this work, the WCA potential featured a depth of the potential well $\epsilon = 1$ kT, an effective size of $\sigma = 0.355\,\mathrm{nm}$, and a cutoff distance $r_{\mathrm{cut}} = 2^{1/6}\sigma$.

The bond between a pair of beads in PMAA chains, is modeled using harmonic potential, described by the expression:

$$U_{\mathrm{bond}}(r) = \frac{\mathrm{K_{bond}}}{2}(r - r_0)^2 \tag{4.11}$$

where $\mathrm{K_{bond}}$ is the stiffness constant of the bond r_0 is the equilibrium bond length. In this work, the stiffness constant $\mathrm{K_{bond}} = 50\ \mathrm{k_B T\,nm^{-2}}$ was assigned to all bonds. The equilibrium length for the backbone and side chain of the PMAA was set to $r_0 = 0.150\,\mathrm{nm}$.

Furthermore, all small ions and the ionized side chains of PMAA engaged in

interactions governed by the Coulomb potential, now expressed as:

$$U_{\text{Coulomb}}(r) = k_{\text{B}} T z_1 z_j \frac{\lambda_B}{r_{ij}} \tag{4.12}$$

where z_i and z_j are the charge numbers of ions i and j, r_{ij} is the distance between them, and λ_B is the Bjerrum length, previously defined in Equation 2.2, building on the Coulombic potential energy introduced in Equation 2.1. For this work, the relative permittivity was set to $\epsilon_r = 78.5$, which is the value for water at $T = 298\,\text{K}$. With these parameters, the Bjerrum length corresponds to 0.71 nm.

4.5.3 Simulation method

Polyelectrolyte ionization was modeled by simulating the acid-base equilibrium through trial moves. Specifically, a protonated group HA may be converted to its deprotonated form A^-, or the other way around, with a corresponding insertion or a removal of an H^+ in the simulation box. [32]

To account for ion exchange between the two compartments, the simulation box was coupled to a virtual reservoir. The exchange of ions between the simulation box and the reservoir also included the insertion and removal of ion pairs consisting of Na^+, Cl^-, $\text{H}^+$and OH^- ions, and was simulated using the Grand-Reaction Monte Carlo method (G-RxMC).[11, 24, 28]

To ensure that the chemical potential of each ion pair in the system matches those in the reservoir, the acceptance probabilities for insertion and deletion of ions are defined based on the chemical potential of the involved ions [30]:

$$P = \min\left\{1, \left(K_{\text{A}} \left(c^{\ominus} V_{\text{box}} N_{\text{A}}\right)^{\bar{\nu}}\right)^{\xi} \prod_i \left[\frac{N_i^0!}{(N_i^0 + \nu_i \xi)!}\right] \times \exp\left(-\frac{\Delta U}{k_{\text{B}} T}\right)\right\} \tag{4.13}$$

where N_{A} is the Avogadro number, N_i is the number of particles i, and ν_i correspond to their stoichiometric coefficient. ΔU corresponds to the change in potential energy between the original and new configurations, and ξ specifies the reaction direction, taking a value of +1 for deprotonation and -1 for protonation.

4.5.4 Simulation protocol

Every simulation cycle included 51 reaction trial moves and 5000 steps of Langevin dynamics integration. Typical simulations involved 16 600 cycles, where $t_{\text{sim}} = 8.3 \times 10^5\,\tau$. Observables and particle coordinates were recorded at intervals of $t_{\text{obs}} = 50\,\tau$ and $t_{\text{coord}} = 250\,\tau$. The sampling was estimated using the slowest-changing observable - the end-to-end distance of the PMAA.

4.5.5 Processing data from simulations

The ΔpH between retentate (pH_{ret}) and permeate (pH_{perm}) was calculated for PMAA concentrations of 1 and 10 g/L with varying NaCl concentrations. The simulations used the same theoretical foundation as the experimental data processing, based on the ideal Donnan equilibrium theory, with the key difference

that ΔpH was computed using a general Equation 2.14 for the distribution ratio of ions. The distribution ratio of Na^+ ions D_{Na^+} is equal to:

$$D_{Na^+} = \frac{c^{ret}_{Na^+}}{c^{perm}_{Na^+}} \tag{4.14}$$

And the distribution ratio of Cl^- ions D_{Cl^-} is equal to:

$$D_{Cl^-} = \frac{c^{ret}_{Cl^-}}{c^{perm}_{Cl^-}} \tag{4.15}$$

The processed simulation data, expressed as distribution ratio D_{Na^+} and D_{Cl^-} and derived ΔpH were compared with experimental results to validate the model.

The simulation script and protocol used in this thesis were developed under the supervision of my advisor. A more detailed description of the simulation model, method and protocol could be found in his doctoral dissertation.[33] All simulations for this work were performed using the software ESPResSo v4.1.4, a molecular dynamics tool designed for soft matter research and originally developed to study charged system, well-suited for simulating polyelectrolyte behavior in this thesis.[34]

5 Results and discussion

5.1 Potentiometric titrations of PMAA

Potentiometric titrations of poly(methacrylic acid) (PMAA) were performed to investigate its pH-dependent ionization behavior, which is governed by the protonation state of its carboxyl groups. At low pH below the pK_A of the PMAA monomer, the −COOH groups are not ionized. In contrast, at high pH values, the −COOH groups become deprotonated, resulting in negatively charged COO^- groups that repel each other, as shown in Figure 5.1. Although PMAA is a weak polyelectrolyte, in the selected experimental pH range of approximately 10, it behaves like a strong polylectrolyte due to near-complete ionization, as indicated in the Figure 5.1.

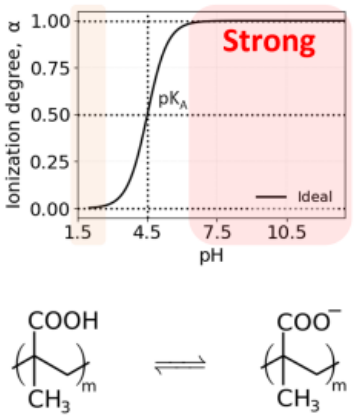

Figure 5.1 The Henderson-Hasselbalch (HH) curve illustrates the degree of ionization of PMAA as a function of pH, with a pK_A of 4.5. The region highlighted in red indicates where PMAA exhibits strong polyelectrolyte behavior. The ionization of carboxyl groups in the side chains of PMAA, consisting of m monomeric units, is shown. Adapted from a figure authored by my advisor Sebastian Pineda Pineda.

The obtained titration curves of PMAA were compared to that of a blank titration, where 2 mL of 0.1 M HCl was titrated with 0.1 M NaOH. The blank titration curve is shown in Figure 5.2 and exhibits a single inflection point at pH 7. The titration curves for PMAA solutions at 10 and 1 g/L, shown in Figures 5.3a and 5.3b, respectively, differ noticeably from the blank titration curve, reflecting the complex ionization behavior of polyelectrolyte. The first inflection point at low pH is not very pronounced, particularly for the 10 g/L solution. That is primarily due to the preparation of the sample solution. Unlike the blank titration, where 2 ml of 0.1 M HCl was used to establish low starting pH, the PMAA solution was prepared by dissolving the polymer directly in water without adding HCl. As a result, the initial pH of the PMAA solutions was not sufficiently acidic. For the 1 g/L solution, the pH saturates after approximately 1 mL of 0.1 M NaOH, indicating complete ionization. The 10 g/L solution stabilizes around 2.5 mL of 0.1 M NaOH. This difference is expected, as the lower concentrated (1 g/L) polyelectrolyte, requires a smaller volume of 0.1 M NaOH to achieve full ionization

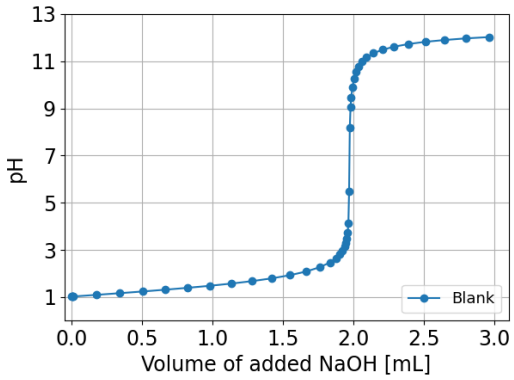

Figure 5.2 The blank titration curve for 2 ml of 0.1 M HCl titrated by 0.1 M NaOH, displays the pH of the solution as a function of the volume of added 0.1 M NaOH, with a visible inflection point at pH 7.

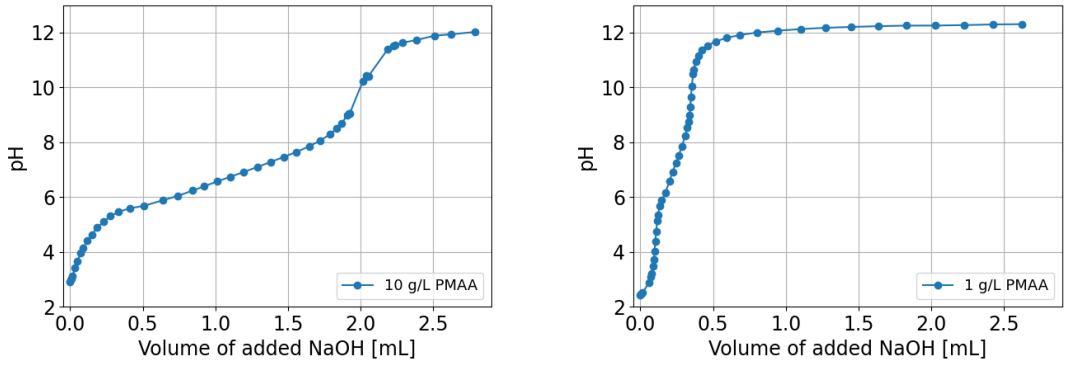

(a) 10 g/L PMAA solution. **(b)** 1 g/L PMAA solution.

Figure 5.3 Titration curves for PMAA solutions at concentrations of (a) 10 g/L and (b) 1 g/L, showing the pH as a function of the volume of 0.1 M NaOH added.

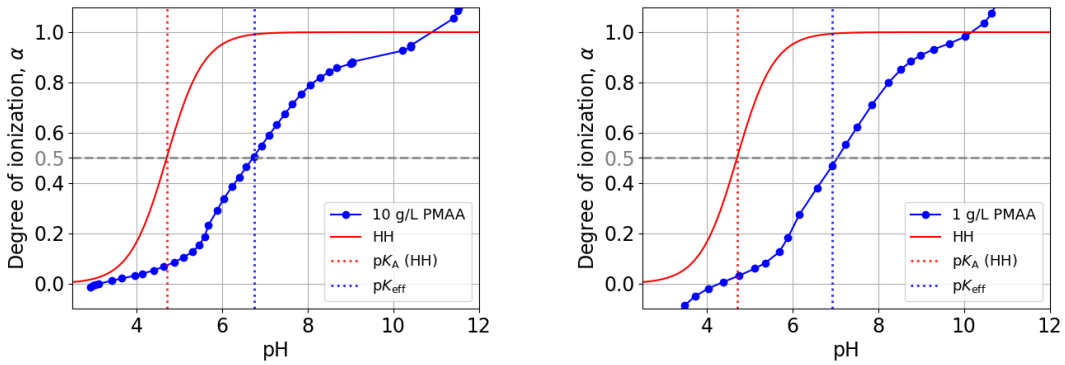

(a) 10g/L PMAA solution. **(b)** 1 g/L PMAA solution.

Figure 5.4 Degree of ionization α of PMAA solutions as a function of solution pH compared with the Henderson-Hasselbalch (HH) curve (Equation 2.5). (a) PMAA at 10 g/L. (b) PMAA at 1 g/L. Vertical lines indicate the pK_A of the PMAA monomer (4.7) and the effective pK_{eff} for each concentration.

compared to the higher concentrated (10 g/L) polyelectrolyte.

To illustrate how the ionization of PMAA varies with pH and concentration, the degree of ionization, α, was plotted against pH as shown in Figures 5.4a and 5.4b. We anticipate that the titration behavior of PMAA solutions deviates from the ideal Henderson-Hasselbalch (HH) curve, due to electrostatic interactions within the polylelectrolyte. Furthermore, we expect pK_{eff} to vary with polymer concentration.

The ideal HH curve assumes a constant pK_A of 4.7. At $\alpha = 0.5$, the effective acidity constant pK_{eff} of PMAA solutions is 7.1 for 1 g/L and 6.7 for 10 g/L, significantly higher than the pK_A of the PMAA monomer (4.7). Notably, the experimental values exceeds $\alpha > 1$ at high pH, likely because the calculation of the charge on the monomeric unit z_{mon} (Equation 4.8) based on pH includes contribution from additional ions from CO_2, that the pH measurement of the titrator cannot distinguish.

In summary, the deviation from the ideal HH curve and the pK_{eff} values determined by our experiments align with our expectations, based on previous experiments and simulation results from the literature.[14, 35, 36] At high polymer concentrations, the polymer chains are closer together, leading to increased electrostatic repulsion between ionized groups. To reduce this repulsion, the polyelectrolyte suppresses ionization, resulting in lower pK_{eff} values compared to lower polymer concentration. Values of α outside the physically meaningful range of $0 - 1$ are disregarded, as they result from the systematic errors due to numerical inaccuracies in pH measurements. The inflection points in Figure 5.4 at pH ≈ 10 could be caused by the uptake of CO_2 from the air during titration.

5.2 Ionization behavior from molecular simulations

Molecular simulations were performed to investigate the pH-dependent ionization of PMAA at concentrations of 1 g/L and 10 g/L, complementing the experimental potentiometric titrations in Section 5.1. To explore the influence of ionic strength on the titration curve, simulations included NaCl concentrations of 10^{-3} M, 10^{-2} M and 10^{-1} M, which were not present in the experimental titrations. Figures 5.5a and 5.5b show the degree of ionization α as a function of pH for PMAA at 10 g/L and 1 g/L, respectively. The figures show simulation results of an ideal system with no interactions between ionizable groups of PMAA and small ions, and an interacting system, which includes the Coulomb interactions. In both systems, the pK_A of the carboxyl groups was set to 4.7. In the interacting system, due to charge regulation on polyelectrolyte chain, the effective acidity constant pK_{eff} is increased as compared to the ideal one, shifting the curves to higher pH.

In the ideal system, the absence of Coulomb interactions result in independent ionization of carboxylic acid groups, producing a single curve for all NaCl concentrations, as in this case, the ionic strength does not influence the ionization. In contrast, the interacting model gives distinct curves for each NaCl concentration, with lower NaCl concentrations shifting the curve to higher pH due to increased repulsions between ionized groups and a higher effective pK_{eff}, while higher NaCl concentrations shift the curve toward lower pH, approaching the ideal model due

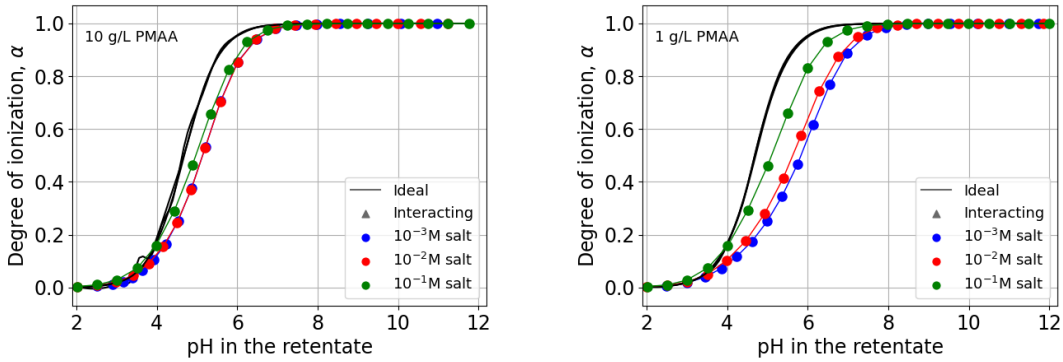

(a) 10 g/L PMAA solution.

(b) 1 g/L PMAA solution.

Figure 5.5 Degree of ionization α of PMAA at concentrations (a) 10 g/L and (b) 1 g/L as a function of solution pH, obtained from molecular simulations. The solid black line represents an ideal system with no interactions, while colored markers indicate results for interacting systems with varying concentration of NaCl.

to enhanced electrostatic screening by the NaCl ions.

For the 10 g/L PMAA solution (Figure 5.5a), the results from interacting simulations in general show smaller shift from the ideal curve, with the curves for 10^{-2} M and 10^{-1} M NaCl almost overlapping. For the 1 g/L PMAA solution (Figure 5.5b), the interacting curves show larger shifts from the ideal curve compared to the 10 g/L, with the 10^{-3} M NaCl curve most shifted to higher pH, reflecting higher effective pK_{eff} due to reduced electrostatic screening at low ionic strength. Therefore, we can conclude that not only pH and ionic strength, but also the polyelectrolyte concentration affect its ionization at a given pH.

5.3 Dialysis of PMAA solutions

The initial dialysis experiments were conducted using PMAA solutions at low degree of ionization (low pH values - around 3 and 4) and dialysate at pH around 10. Experiments with PMAA at a higher pH of around 8 with different PMAA concentrations produced uncertain results, as described in Section 4.3.2. We consider these early findings unreliable, as they came before our optimized protocol, which later ensured pH stability and measurement consistency. Nevertheless, they provided important inputs to understand under which conditions we could obtain more reliable results.

c_{PMAA} (g/L)	c_{NaCl} (mol/L)	pH_{perm} 0 h	pH_{perm} 72 h	pH_{ret} 0 h	pH_{ret} 72 h
9.900	9.9×10^{-4}	10.50	6.40	2.490	5.17
9.952	10^{-3}	10.10	6.490	3.0	5.180
9.952	10^{-3}	9.90	6.220	2.990	5.160
10.210	10^{-3}	9.892	5.302	2.026	4.573
10.210	10^{-3}	9.845	4.629	2.110	4.109
10.210	10^{-3}	9.660	6.324	4.369	5.232
10.210	10^{-3}	9.680	6.50	4.360	5.10
0.988	10^{-3}	9.613	8.462	8.048	8.157
0.988	10^{-3}	9.571	8.871	8.150	8.212
3.298	10^{-3}	9.50	7.20	8.050	7.70
3.298	10^{-3}	9.470	9.470	8.012	7.862

Table 5.1 Overview of the preliminary dialysis results from optimization of the protocol. The table presents pH values of the permeate (pH_{perm}) and retentate (pH_{ret}) for different PMAA and NaCl concentrations (c_{PMAA} and c_{NaCl}), measured initially (0 hours) and after 72 hours.

5.3.1 Theoretical predictions using the ideal Donnan theory

Theoretical ΔpH values were calculated using the ideal Donnan equilibrium theory, as detailed in Section 4.3.4, for $c_{PMAA} = 1$ and 10 g/L, corresponding to molar concentrations of monomeric units (c_A) of 0.0116 M and 0.116 M, respectively. The ionic strength of the permeate (I_{perm}) was computed using Equation 4.1, based on c_{NaCl} and $[OH^-]$ from the initial permeate pH. The distribution ratio (D_+) was determined using Equations 4.2, assuming complete PMAA ionization ($\alpha \approx 1$) at pH 10, and ΔpH was calculated from Equation 4.4. These predictions, plotted as functions of I_{perm}, are used for comparison with experimental results in Section 5.3.2.

5.3.2 Experimental ΔpH measurements during dialysis

Optimization of dialysis duration

Expecting that dialysis of PMAA solutions would reach equilibrium over hours to days, we conducted preliminary experiments using lower concentration of 1 g/L to save the valuable polymer sample. These experiments, performed over 4 days with measurements taken every 12 hours, measured the pH of both the retentate and permeate solutions over time, with results shown in Figure 5.6. The experiments were performed using PMAA solutions at a concentration of 1 g/L, with an initial pH around 3.6, dialyzed against NaCl solution, $c_{NaCl} = 10^{-3}$ M, with an initial pH set to 10. Significant changes in the ΔpH were observed after 24 and 60 hours of dialysis. After 60 hours, the ΔpH values remained stable.

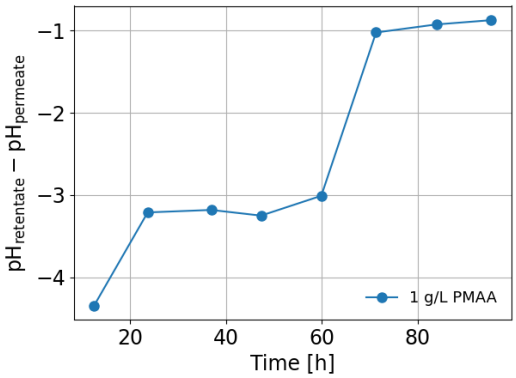

Figure 5.6 Time-dependent ΔpH for preliminary dialysis experiments with PMAA at 1 g/L (initial pH 3.6) dialyzed against NaCl at 0.001 M (initial pH 10). Measurements were taken every 12 hours over 4 days, showing stabilization after 60 hours, to determine the optimal dialysis duration of 72 hours.

Based on these results, a convenient dialysis duration of 72 hours was selected for the upcoming experiments.

Equilibrium ΔpH from optimized dialysis experiments

The optimized dialysis experiments were performed to observe the behavior of PMAA solutions under varying NaCl dialysate concentrations and were set up carefully to ensure reliable results and check that our protocol worked as intended. To ensure reliability and consistency of the measured values, dialysis setups were prepared in duplicate, as detailed in Chapter 4. Measured variables were the concentrations of PMAA (c_{PMAA}) and NaCl (c_{NaCl}), as well as the pH of the permeate ($\mathrm{pH_{perm}}$) and retentate ($\mathrm{pH_{ret}}$). These pH values were measured at start of the dialysis (0 h), and after 72 h.

The results of these experiments are summarized in Table 5.2, which shows the initial and equilibrium pH values with corresponding c_{PMAA} and c_{NaCl} for each experimental setup, with all measurements performed in duplicate. Although the initial pH of permeate and retentate was intended to be set to 10 for all setups, achieving and maintaining this value for PMAA concentration 10 g/L turned out to be challenging due to the buffering activity of PMAA, resulting in deviations of up to 0.57 pH units at 0 h. In contrast, for the lower concentration of 1 g/L PMAA, the initial pH was more stable and closer to the target value. These findings indicate that for higher PMAA concentrations, more precise pH adjustment at a slightly higher pH may be required to ensure consistent starting conditions. However, based on the data obtained from the titration, the ionization degree of PMAA at this pH range is expected to exceed 0.9, indicating that the PMAA remains highly ionized despite these fluctuations.

After 72 hours, pH shifts were recorded in both permeate and retentate compared to initial pH. In the permate, these shifts were relatively small and are most probably due to carbonization, given the set basic pH. In contrast, the retentate showed more pronounced pH shifts, particularly at higher PMAA concentration 10 g/L and lower NaCl concentration (around 10^{-3} M), corresponding to lower ionic strength. These results support our expectations, that the observed pH

c_{PMAA}	c_{NaCl}	$\mathrm{pH}_{\mathrm{perm}}$		$\mathrm{pH}_{\mathrm{ret}}$	
(g/L)	**(mol/L)**	**0 h**	**72 h**	**0 h**	**72 h**
9.947	9.4×10^{-4}	10.244	9.770	9.834	9.040
9.947	9.4×10^{-4}	10.532	10.060	9.790	9.250
9.648	9.83×10^{-3}	10.135	9.895	9.470	9.320
9.648	9.83×10^{-3}	10.182	9.805	9.479	9.230
9.648	9.83×10^{-2}	10.080	9.874	9.470	9.751
9.648	9.83×10^{-2}	10.082	9.850	9.430	9.718
0.963	9.9×10^{-4}	10.997	10.961	11.695	10.667
0.963	9.9×10^{-4}	11.005	10.998	11.710	10.672
1.00	9.997×10^{-3}	10.017	9.978	9.974	9.896
1.00	9.997×10^{-3}	10.017	10.008	9.957	9.901
1.00	10^{-1}	9.932	9.952	9.865	9.943
1.00	10^{-1}	9.670	9.949	9.810	9.918

Table 5.2 Overview of the optimized dialysis results. The table presents pH values of the retentate and permeate over 72 hours for various PMAA and NaCl concentrations (c_{PMAA} and c_{NaCl}), measured initially (0 hours) and after 72 hours.

changes in the retentate are primarily driven by the Donnan effect, which are more pronounced at higher PMAA concentrations and lower ionic strength of the permeate. Meanwhile, the relatively stable pH in the permeate - likely affected only by carbonization - confirms the effectiveness of the experimental protocol in minimizing the carbonization at high pH.

Comparison of experimental and theoretical ΔpH

We anticipated that the ideal Donnan theory would not perfectly match the experimental data, but we were unsure about the extent of the deviation. Therefore, from data summarized in Table 5.2, experimental ΔpH, calculated using Equation 2.18, were plotted in Figure 5.7 against ionic strength I_{perm} (logarithmic scale) calculated for each system using Equation 4.1 (as described in Section 4.3.3). These experimental ΔpH values are compared to theoretical ΔpH values calculated from the Donnan equilibrium theory (Section 4.3.4), using Equations 4.2 and 4.4, assuming complete PMAA ionization at the initial pH of 10, for $c_{\mathrm{PMAA}} = 1$ and $10\,\mathrm{g/L}$.

On the log scale, the difference between experimental and theoretical ΔpH becomes more pronounced at low ionic strengths ($I_{\mathrm{perm}} \leq 10^{-2}\,\mathrm{M}$) especially for $c_{\mathrm{PMAA}} = 10\,\mathrm{g/L}$. For $c_{\mathrm{PMAA}} = 1\,\mathrm{g/L}$, the difference is also evident at low I_{perm} though less significant. The ideal theory accurately predicts ΔpH only for $c_{\mathrm{PMAA}} = 1\,\mathrm{g/L}$ at $I_{\mathrm{perm}} = 10^{-1}\,\mathrm{M}$, where experimental and theoretical values align closely, indicating the ideal theory applies, when the polyelectrolyte concentration is low and the ionic strength of permeate is high. Specifically, for $c_{\mathrm{PMAA}} = 1\,\mathrm{g/L}$, the molar concentration of monomeric units (c_{A}) corresponds to $0.0116\,\mathrm{M}$

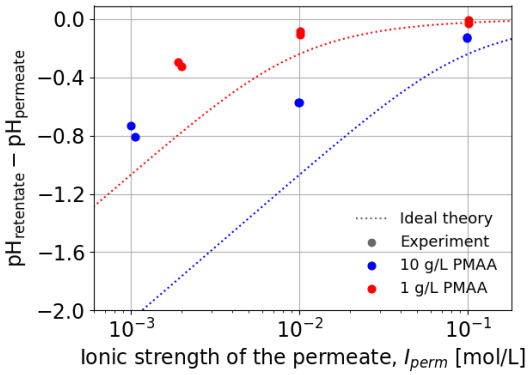

Figure 5.7 ΔpH as a function of the ionic strength of the permeate I_{perm} on a logarithmic scale at various polymer concentrations, at $\text{pH}_{\text{ret}} \approx 10$. The dotted lines correspond to the ideal curve from Donnan theory for $\alpha = 1$, and the experimental data are presented as markers in duplicates for different ionic strengths of the permeate and concentrations of PMAA.

(Section 4.3.4), which is lower than the ionic strength of 10^{-1} M.

Although the experimental data do not align with the theoretical curves, they follow the general trend, deviating more significantly as the difference in ΔpH increases. This trend suggests that although the ideal theory does not perfectly match the experimental data, it still reflects the overall behavior of the system, serving as a useful approximation.

5.3.3 Comparison of experiments and simulations

Our hypothesis is that simulations including interacting systems should closely reproduce experimental ΔpH values. In contrast, ideal simulations, which neglect these interactions, align with the predictions of ideal Donnan theory.[24]

To test this hypothesis, we compare experimental ΔpH measurements for PMAA concentrations of 10 and 1 g/L, as shown in Figures 5.8 and 5.9, respectively, with results from simulations. Both experiments and simulations were conducted at three NaCl concentrations: 10^{-3}, 10^{-2} and 10^{-1} M. The simulation data include three distinct datasets: an ideal system, where interactions are neglected, an interacting system, where full intermolecular interactions are included, and ΔpH calculated from the distribution of Na^+ions and Cl^- ions for both the ideal and interacting systems. We expect the experimental ΔpH data to be predicted by the distribution coefficient of Na^+ ions, which is inversely proportional to that of Cl^- ions in both systems. However, preliminary analysis revealed deviations, particularly at low salt concentrations ($c_{\text{NaCl}} = 10^{-3}$ M for both 10 and 1 g/L, and $c_{\text{NaCl}} = 10^{-2}$ M for 10 g/L), where finite size effects in the simulations lead to unusual curve patterns.[37]

These finite size effects primarily come from the limited number of Cl^-ions in the simulation box, especially at low salt concentrations.[37] To reduce these issues, increasing the simulation box size would allow for a larger number of Cl^-ions, which would also require much longer simulation times, particularly for the interacting system, where the dynamics require extended equilibration runs. However, increasing system size and simulation duration is computationally

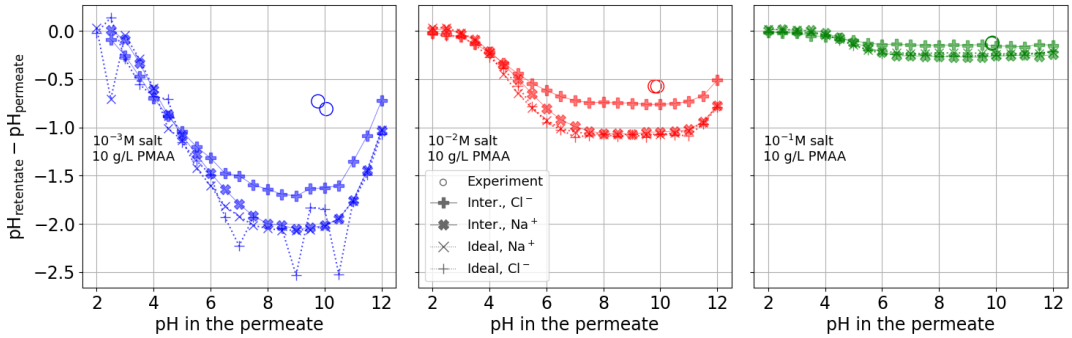

Figure 5.8 Comparison of experimental and simulation data for the dependence of ΔpH on the pH in the retentate at a PMAA concentration of 10 g/L. Each subplot corresponds to a different NaCl concentration (c_{NaCl}), as indicated in each subplot. The ideal and interacting simulation data are shown for the distribution of Na^+ and Cl^- ions, with different markers distinguishing the two data sets. Experimental data are presented in duplicates for each subplot.

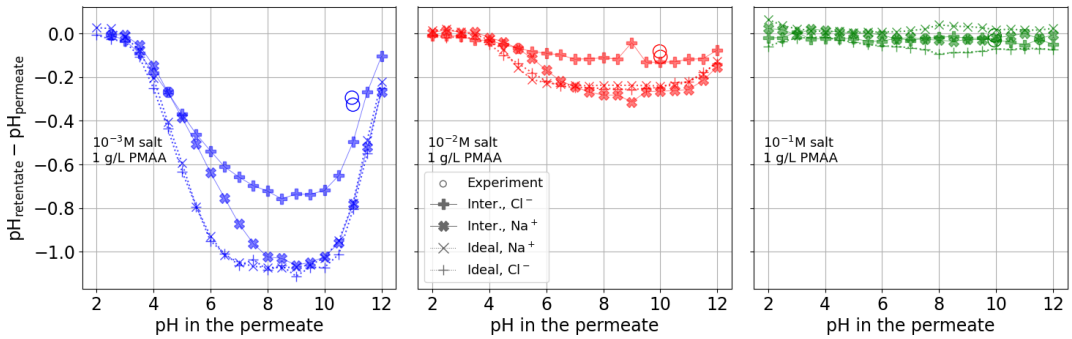

Figure 5.9 Comparison of experimental and simulation data for the dependence of ΔpH on the pH in the retentate at a PMAA concentration of 1 g/L. Each subplot corresponds to a different NaCl concentration (c_{NaCl}), as indicated in each subplot. The ideal and interacting simulation data are shown for the distribution of Na^+ and Cl^- ions, with different markers distinguishing the two data sets. Experimental data are presented in duplicates for each subplot.

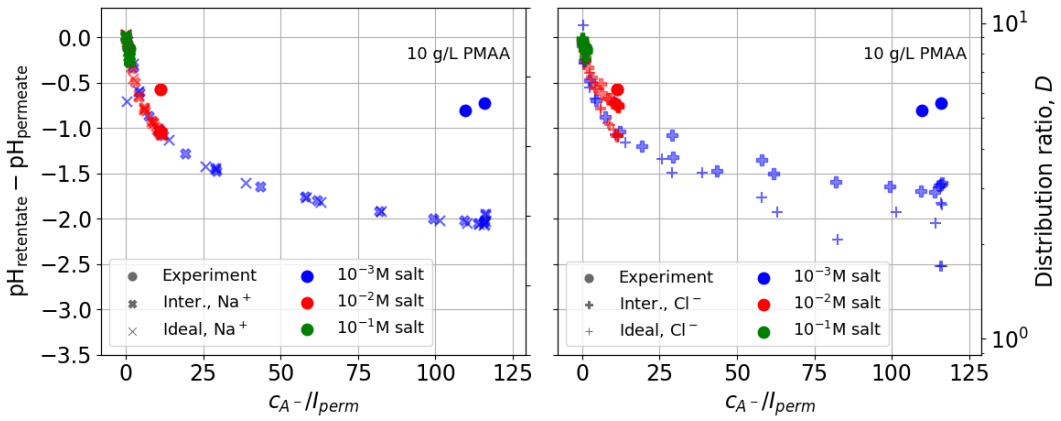

Figure 5.10 Comparison of experimental and simulation data (ideal and interacting) showing the dependence of ΔpH (left y-axis) and D_+ (right y-axis) on the ratio $c_\mathrm{A}/I_\mathrm{perm}$ at a fixed PMAA concentration of 10 g/L. Each subplot corresponds to a different ion distribution ratio: the left for Na^+ ions, and the right for Cl^- ions. Colors represent different NaCl concentrations. Simulation data include both ideal and interacting models, with different markers for each. Experimental data are presented in duplicates in both subplots.

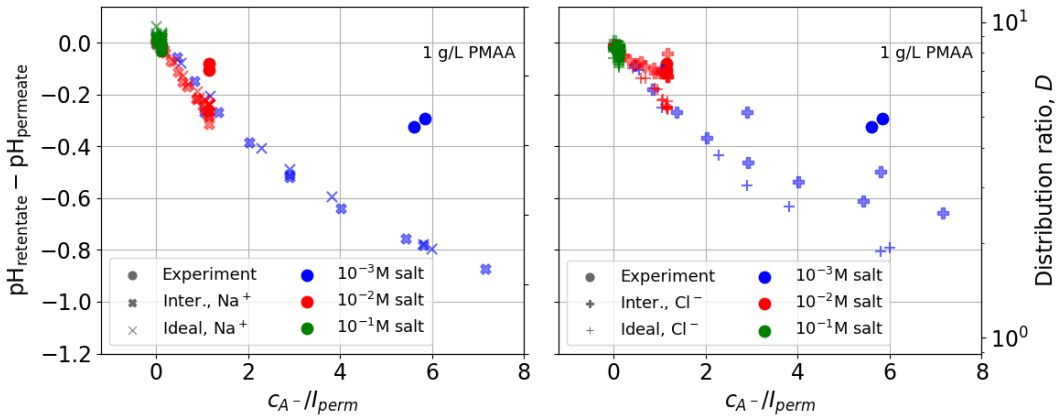

Figure 5.11 Comparison of experimental and simulation data (ideal and interacting) showing the dependence of ΔpH (left y-axis) and D_+ (right y-axis) on the ratio $c_\mathrm{A}/I_\mathrm{perm}$ at a fixed PMAA concentration of 1 g/L. Each subplot corresponds to a different ion distribution ratio: the left for Na^+ ions, and the right for Cl^- ions. Colors represent different NaCl concentrations. Simulation data include both ideal and interacting models, with different markers for each. Experimental data are presented in duplicates in both subplots.

demanding, making these simulations too time-consuming for the thesis deadline.

Interestingly, the ΔpH of the interacting system derived from the distribution of Cl^- ions between the retentate and permeate, aligns more closely with experimental values. In contrast, ΔpH derived from Na^+ ion distribution tends to follow the ideal simulation curves, challenging the expected equal distribution of cations and anions.

The subplots in Figures 5.10 and 5.11 present the comparison of experimental and simulation data for the dependence of ΔpH and D_+ on the ratio c_A/I_{perm} at fixed polymer concentration of 10 g/L and 1 g/L. In these subplots, the left panel displays data calculated from the distribution ratio of Na^+ while the right panel shows data calculated from Cl^- ion distributions. These results are expected to validate our findings from the previous comparisons (Figures 5.8 and 5.9). For a given c_{PMAA}, data points across different c_{NaCl} values are expected to align on a single curve.

The data obtained from simulations generally follow the trend of one single curve. However, deviations from this curve are observed, which could be caused by the finite-size effect[37], or by the asymmetric roles of monovalent cations and anions in the studied system. Our current simulation results do not allow us to distinguish these two possible causes. They could be distinguished based on simulations of bigger systems, where the finite-size effects are suppressed. However, such simulations could not be completed before submitting the thesis. At a salt concentration of 10^{-1} M, both experimental and simulation data align closely for both 10 g/L and 1 g/L polymer concentration. In contrast, at lower salt concentration of 10^{-2} M, deviations from the single curve become apparent, particularly for the interacting simulation data obtained from Cl^- distribution, that surprisingly align more with the experimental data, especially at 1 g/L polymer concentration. For the lowest concentration of salt 10^{-3} M the simulation data deviate the most from experiments. These results are consistent with earlier figures examining the dependence of ΔpH on pH in the retentate, where similar interactions were observed.

6 Conclusions

The primary goal of this thesis was to experimentally quantify the Donnan effect during dialysis of polyelectrolyte solutions, using poly(methacrylic acid) (PMAA) as a model system. A key objective was to develop a reliable and reproducible experimental protocol measuring pH differences across a dialysis membrane. This protocol, detailed in Section 4.3, has been successfully established, enabling systematic investigation of PMAA behavior under varying pH and ionic strength conditions. However, the optimization process required considerable time and effort, which limited the number of reliable data that could be collected using the completed protocol.

The experimental results from dialysis demonstrated measurable pH differences due to the Donnan effect, confirming that dialysis works as a basic method to study polyelectrolytes. Comparisons with theoretical predictions from ideal Donnan equilibrium theory at high pH (where degree of ionization of the PMAA was approximately 1) showed that experimentally measured values were effectively lower than the predictions from ideal theory, especially at higher polymer concentration and lower salt concentration, where the Donnan effect was the most pronounced. Despite these deviations, the experimental data and simulations exhibited quantitative agreement in the trends predicted by ideal Donnan theory. Since the ideal Donnan theory does not account for any interactions in the system, these results show, that the interactions are key under such conditions.

To further explore this, predictions from molecular simulations were employed, although they are not the primary focus of this thesis. While we did not explicitly verify this, we expect that the results of simulations without interactions would align with the predictions of the ideal Donnan model, as the ideal simulation model was derived from the ideal theory.[24, 28] At the same time, we expected simulation results including interactions to more accurately capture the experimentally observed ΔpH, particularly ΔpH calculated based on the distribution of Na^+ ions between the retentate and permeate. However, this was not fully achieved, potentially due to simplifications in the model that may not accurately reflect the system. We also dealt with the finite-size effect – an issue we were unable to fully resolve within the time constraints of this project, as increasing the simulation box size would require significantly more computational time, especially for interacting system.

Interestingly, ΔpH derived from the distribution of Cl^- ions between the retentate and permeate in the interacting simulations unexpectedly aligned more closely with experimentally measured values, despite not matching them entirely. In contrast, ΔpH derived from Na^+ ion distribution followed the trend of the curve from the ideal systems, deviating further from experimental observations. This suggest the model may be on the right track for accurately representing non-ideal polyelectrolyte behavior, but more studies are needed to validate these findings. On the other hand, the consistent agreement at 10^{-1} M salt across both polymer concentrations, where ΔpH is small, indicates that ideal models are sufficient under these conditions.

6.1 Outlooks

This thesis provides a starting point for further studying the Donnan effect in polyelectrolyte dialysis. The findings give a foundation for extending this work to more complex systems, such as proteins, which are widely used in pharmaceutical applications at high concentrations like monoclonal antibody production, that exhibit pronounced Donnan effect.[2]

Future studies will first explore the Donnan effect across a wider range of pH conditions for both polymer and dialysate solutions, as well as varying ionic strength, to deepen the understanding of polyelectrolyte behavior in dialysis under varying experimental conditions. These investigations are directly correlated to protein dialysis, where precise control of pH is critical for maintaining protein stability and quality during industrial processes like ultrafiltration/diafiltration (UF/DF). By first improving our understanding of the Donnan effect in simpler polyelectrolyte systems like PMAA under these challenging conditions, we can potentially adapt and optimize the dialysis protocol for proteins, addressing the pronounced deviations from theoretical predictions that occur at high protein concentrations. We also plan to use NMR spectroscopy to directly quantify Na^+ and Cl^- ion distributions across the dialysis membrane, providing another set of data to validate experimentally measured deviations from ideal Donnan predictions and complement our existing experimental methods.

References

[1] Murugappan Muthukumar. *Physics of Charged Macromolecules: Synthetic and Biological Systems*. Cambridge University Press, 2023.

[2] Till Briskot et al. "Modeling the Gibbs–Donnan effect during ultrafiltration and diafiltration processes using the Poisson–Boltzmann theory in combination with a basic Stern model". In: *Journal of Membrane Science* 648 (2022), p. 120333. ISSN: 0376-7388. DOI: https://doi.org/10.1016/j.memsci.2022.120333. URL: https://www.sciencedirect.com/science/article/pii/S0376738822000801.

[3] Andrey V. Dobrynin. "Theory and simulations of charged polymers: From solution properties to polymeric nanomaterials". In: *Current Opinion in Colloid & Interface Science* 13.6 (2008), pp. 376–388. ISSN: 1359-0294. DOI: https://doi.org/10.1016/j.cocis.2008.03.006. URL: https://www.sciencedirect.com/science/article/pii/S1359029408000411.

[4] Mitsuru Nagasawa. "Advances in Chemical Physics, Volume 158". In: *Advances in Chemical Physics*. Vol. 158. John Wiley & Sons, Inc., 2015. ISBN: 9781119057086. DOI: 10.1002/9781119057338. URL: https://doi.org/10.1002/9781119057338.

[5] Paul Higgs and Elie Raphael. "Conformation changes of a polyelectrolyte chain in a poor solvent". In: *Journal de Physique I* 1.1 (1991), pp. 1–7. DOI: 10.1051/jp1:1991111. URL: https://hal.science/jpa-00246298.

[6] Peter Atkins and Julio de Paula. *Physical Chemistry*. 8th edition. W. H. Freeman, 2006. ISBN: 978-0-7167-8759-4.

[7] Guangming Liu, Drew Parsons, and Vincent Stuart James Craig. "Reentrant swelling and redissolution of polyelectrolytes arises from an increased electrostatic decay length at high salt concentrations". In: *Journal of Colloid and Interface Science* 579 (2020), pp. 369–378. ISSN: 0021-9797. DOI: https://doi.org/10.1016/j.jcis.2020.06.072. URL: https://www.sciencedirect.com/science/article/pii/S0021979720308171.

[8] Sarkyt E. Kudaibergenov. *Polyampholytes: Past, Present, Perspectives*. English. Almaty, 2021.

[9] Johan R C van der Maarel. *Introduction to Biopolymer Physics*. WORLD SCIENTIFIC, 2007. DOI: 10.1142/6644.

[10] Pablo M. Blanco et al. "Unusual Aspects of Charge Regulation in Flexible Weak Polyelectrolytes". In: *Polymers* 15.12 (2023). ISSN: 2073-4360. DOI: 10.3390/polym15122680. URL: https://www.mdpi.com/2073-4360/15/12/2680.

[11] Sebastian P. Pineda et al. "Patchy Charge Distribution Affects the pH in Protein Solutions during Dialysis". In: *Langmuir* 41.8 (2025). PMID: 39964136, pp. 5387–5398. DOI: 10.1021/acs.langmuir.4c04942. eprint: https://doi.org/10.1021/acs.langmuir.4c04942. URL: https://doi.org/10.1021/acs.langmuir.4c04942.

[12] Magnus Ullner and Clifford E. Woodward. “Simulations of the Titration of Linear Polyelectrolytes with Explicit Simple Ions: Comparisons with Screened Coulomb Models and Experiments”. In: *Macromolecules* 33.19 (2000), pp. 7144–7156. DOI: 10.1021/ma991056k. eprint: https://doi.org/10.1021/ma991056k. URL: https://doi.org/10.1021/ma991056k.

[13] Sebastian P. Pineda et al. “Charge Regulation Triggers Condensation of Short Oligopeptides to Polyelectrolytes”. In: *JACS Au* 4.5 (2024), pp. 1775–1785. DOI: 10.1021/jacsau.3c00668. eprint: https://doi.org/10.1021/jacsau.3c00668. URL: https://doi.org/10.1021/jacsau.3c00668.

[14] R. Arnold. “The titration of polymeric acids”. In: *Journal of Colloid Science* 12.6 (1957), pp. 549–556. ISSN: 0095-8522. DOI: https://doi.org/10.1016/0095-8522(57)90060-0. URL: https://www.sciencedirect.com/science/article/pii/0095852257900600.

[15] J.P. Hervás Pérez, B. López-Ruiz, and E. López-Cabarcos. “Synthesis and characterization of microparticles based on poly-methacrylic acid with glucose oxidase for biosensor applications”. In: *Talanta* 149 (2016), pp. 310–318. ISSN: 0039-9140. DOI: https://doi.org/10.1016/j.talanta.2015.11.053. URL: https://www.sciencedirect.com/science/article/pii/S0039914015305051.

[16] Mikael Lund and Bo Jönsson. “Charge regulation in biomolecular solution”. In: *Quarterly Reviews of Biophysics* 46.3 (2013), pp. 265–281. DOI: 10.1017/S003358351300005X.

[17] R. Lunkad et al. “Role of pKA in Charge Regulation and Conformation of Various Peptide Sequences”. In: *Polymers* 13.2 (Jan. 2021), p. 214. DOI: https://doi.org/10.3390/polym13020214.

[18] Thermo Fisher Scientific. *Recombinant Protein Information*. https://www.thermofisher.com/cz/en/home/life-science/cell-culture/cell-culture-learning-center/recombinant-protein-information.html. Accessed: 2025-04-27.

[19] “Overview of Membrane Science and Technology”. In: *Membrane Technology and Applications*. John Wiley & Sons, Ltd, 2023. Chap. 1, pp. 1–17. ISBN: 9781119686026. DOI: https://doi.org/10.1002/9781119686026.ch1. eprint: https://onlinelibrary.wiley.com/doi/pdf/10.1002/9781119686026.ch1. URL: https://onlinelibrary.wiley.com/doi/abs/10.1002/9781119686026.ch1.

[20] Howard DeVoe. Accessed: 2025-04-22, CC BY 4.0 License. n.d. URL: https://chem.libretexts.org/Bookshelves/Physical_and_Theoretical_Chemistry_Textbook_Maps/DeVoes_Thermodynamics_and_Chemistry/12%3A_Equilibrium_Conditions_in_Multicomponent_Systems/12.07%3A_Membrane_Equilibria.

[21] Mahmoud Shaban et al. “Membrane Separation Processes: Principles, Structures, Materials, and Future Prospects”. In: *Advances in Desalination Insights*. Ed. by Huijin Xu et al. Rijeka: IntechOpen, 2024. Chap. 4. DOI: 10.5772/intechopen.1006562. URL: https://doi.org/10.5772/intechopen.1006562.

[22] Geoffrey Allen and John C. Bevington, eds. *Comprehensive Polymer Science and Supplements*. English. 1st. Also available online as eBook ISBN: 978008096701. Pergamon, 1996. ISBN: 9780080426815.

[23] G. R. Bolton et al. "Effect of protein and solution properties on the Donnan effect during the ultrafiltration of proteins". In: *Biotechnology Progress* 27.1 (Jan. 2011). Epub 2010 Dec 3, pp. 140–152. DOI: 10.1002/btpr.523.

[24] Jonas Landsgesell et al. "Grand-Reaction Method for Simulations of Ionization Equilibria Coupled to Ion Partitioning". In: *Macromolecules* 53.8 (Apr. 2020), pp. 3007–3020. DOI: 10.1021/acs.macromol.0c00260. URL: http://dx.doi.org/10.1021/acs.macromol.0c00260.

[25] Jiří Kolafa. *Molekulové modelování a simulace*. Ústav Fyzikální chemie, VŠCHT Praha. Accessed April 23, 2025. May 22, 2023. URL: https://old.vscht.cz/fch/cz/pomucky/kolafa/molsim-tisk.pdf.

[26] Riccardo Baron et al. "Comparison of Atomic-Level and Coarse-Grained Models for Liquid Hydrocarbons from Molecular Dynamics Configurational Entropy Estimates". In: *The journal of physical chemistry. B* 110 (May 2006), pp. 8464–73. DOI: 10.1021/jp055888y.

[27] Sebastian Kmiecik et al. "Coarse-Grained Protein Models and Their Applications". In: *Chemical Reviews* 116.14 (2016), pp. 7898–7936. DOI: 10.1021/acs.chemrev.6b00163.

[28] David Beyer et al. "Correction to "Grand-Reaction Method for Simulations of Ionization Equilibria Coupled to Ion Partitioning"". In: *Macromolecules* 55.3 (2022), pp. 1088–1088. DOI: 10.1021/acs.macromol.1c02672. eprint: https://doi.org/10.1021/acs.macromol.1c02672. URL: https://doi.org/10.1021/acs.macromol.1c02672.

[29] Magnus Ullner and Bo Jönsson. "A Monte Carlo Study of Titrating Polyelectrolytes in the Presence of Salt". In: *Macromolecules* 29.20 (1996), pp. 6645–6655. DOI: 10.1021/ma960309w.

[30] David Beyer et al. "pyMBE: The Python-based molecule builder for builder for ESPResSo". In: *The Journal of Chemical Physics* 161.2 (July 2024), p. 022502. ISSN: 0021-9606. DOI: 10.1063/5.0216389. eprint: https://pubs.aip.org/aip/jcp/article-pdf/doi/10.1063/5.0216389/20043779/022502_1_5.0216389.pdf. URL: https://doi.org/10.1063/5.0216389.

[31] Turner Jr. Alfrey and Herbert Morawetz. "Amphoteric Polyelectrolytes. I. 2-Vinylpyridine—Methacrylic Acid Copolymers1,2". In: *Journal of the American Chemical Society* 74.2 (1952), pp. 436–438. DOI: 10.1021/ja01122a046. eprint: https://doi.org/10.1021/ja01122a046. URL: https://doi.org/10.1021/ja01122a046.

[32] W. R. Smith and B. Tříska. "The reaction ensemble method for the computer simulation of chemical and phase equilibria. I. Theory and basic examples". In: *Journal of Chemical Physics* 100.4 (1994), pp. 3019–3027. DOI: 10.1063/1.466443.

[33] Sebastian Pineda Pineda. en. PhD thesis. Prague: Charles University, 2025, in preparation.

[34] Florian Weik et al. “ESPResSo 4.0 – an extensible software package for simulating soft matter systems”. In: *The European Physical Journal Special Topics* 227.14 (Mar. 2019), pp. 1789–1816. ISSN: 1951-6401. DOI: 10.1140/epjst/e2019-800186-9. URL: https://doi.org/10.1140/epjst/e2019-800186-9.

[35] Lucie Nová, Filip Uhlík, and Peter Košovan. “Local pH and effective pKA of weak polyelectrolytes – insights from computer simulations”. In: *Phys. Chem. Chem. Phys.* 19 (22 2017), pp. 14376–14387. DOI: 10.1039/C7CP00265C. URL: http://dx.doi.org/10.1039/C7CP00265C.

[36] Felix A. Plamper et al. “Synthesis, Characterization and Behavior in Aqueous Solution of Star-Shaped Poly(acrylic acid)”. In: *Macromolecular Chemistry and Physics* 206.18 (2005), pp. 1813–1825. DOI: https://doi.org/10.1002/macp.200500238. eprint: https://onlinelibrary.wiley.com/doi/pdf/10.1002/macp.200500238. URL: https://onlinelibrary.wiley.com/doi/abs/10.1002/macp.200500238.

[37] Paul Hebbeker et al. “Finite-Size Effects in Simulations of Chemical Reactions”. In: *ChemRxiv* (2023). DOI: 10.26434/chemrxiv-2023-n2g58.